ISSN 1810-2328, Journal of Engineering Thermophysics, 2018, Vol. 27, No. 4, pp. 456–473. © Pleiades Publishing, Ltd., 2018.

# Variable Fluid Property Effect on Heat Transfer and Frictional Flow Characteristics of Water Flowing through Microchannel

**R. Kumar[1]* and S. P. Mahulikar[2]****

[1]*Department of Mechanical Engineering, Dr. B. R. Ambedkar National Institute of Technology, Jalandhar, 144011 India*

[2]*Department of Aerospace Engineering, Indian Institute of Technology, Bombay, P.O. IIT Powai, Mumbai, 400076 India*

Received December 21, 2016

**Abstract**—The effects of temperature-dependent viscosity and thermal conductivity on heat transfer and frictional flow characteristics of water flowing through a microchannel are numerically investigated in this work. The hydrodynamically and thermally developing flow with no-slip, no-temperature jump, and constant wall heat flux boundary condition is numerically studied using 2D continuum-based conservation equations. A significant deviation in Nusselt number from conventional theory is observed due to flattening of axial velocity profile due to temperature-dependent viscosity variation. The Nusselt number shows a significant deviation from conventional theory due to flattening of the radial temperature profile due to temperature-dependent thermal conductivity variation. It is noted that the deviation in Nusselt number from conventional theory is maximum for combined temperature-dependent viscosity and thermal conductivity variations. The effects of temperature-dependent viscosity and thermal conductivity on the Fanning friction factor are also investigated. Additionally, the effects of variable fluid properties on Poiseuille number, Prandtl number, and Peclet number are also investigated.

**DOI:** 10.1134/S1810232818040082

## 1. INTRODUCTION

Fluid flow and heat transfer in microchannels are an important area of research due to its critical uses in a large number of engineering applications and scientific disciplines, such as electronics and microelectronics, microheater and microscale heat exchangers, micropower generation, chemical separation processes, biochemistry, automotive vehicles, thin film deposition technologies, materials processing and aerospace technology, etc. The high-temperature gradients in microconvection due to permissible high heat flux and low Reynolds number flow result in additional physical mechanisms due to variations in fluid properties. Therefore, the aim of the present investigation is to enhance the understanding of microconvection physics, which can lead to identifying additional physical mechanisms, and their role in flow and heat transfer characteristics.

The property ratio method and reference temperature method were used to find the correction of Nusselt number for convection in conventional tubes [1]. An asymptotic theory method was proposed by Herwig [2] to analyze the influence of variable properties on a laminar fully developed pipe flow for small perturbations in temperature. Since the asymptotic theory method was based on a linear temperature dependence of the fluid properties, it failed to provide reasonable prediction at large heat flux. Later, Herwig et al. [3] investigated the effect of temperature-dependent fluid properties on momentum and heat transfer by using the asymptotic method that had been used by Herwig [2] with constant wall heat flux (CWHF) thermal boundary condition, $q''_w$ = constant. However, the constant wall temperature (CWT) thermal boundary condition, $T_w$ = constant, is used [3]. It is borrowed from the macroscale that the role of temperature-dependent viscosity variation is to distort the axial velocity profile over the cross section,

*E-mail: rajank@nitj.ac.in

**E-mail: spm@aero.iitb.ac.in

thereby altering the Nusselt number from the expected value for constant fluid properties [4, 5]. The allowable temperature range over the cross section for common working liquids (like de-ionized water) is limited within the boiling and freezing temperatures and the change in $Nu$ based on reported correlations is not significant enough to explain the experimentally observed deviations in microscale convection characteristics. Tunc and Bayazitoglu [6] solved hydrodynamically and thermally developed laminar flow in micro-tubes with uniform heat flux boundary conditions by an integral transform technique. Tunc and Bayazitoglu [7] solved the hydrodynamically developed laminar flow in micro-tubes with uniform heat flux and uniform temperature boundary conditions by an integral transform technique. They solved an energy equation with the temperature jump boundary condition at the wall analytically, and viscous dissipation effects were also included. Palm [8] and Mahulikar et al. [9] presented the literature survey on microscale heat transfer with single-phase laminar forced liquid convection. The experimental and numerical studies of microflow revealed significant deviation from the known classical theory for conventionally sized channels due to scaling effects. Ameel et al. [10], Guo and Li [11], and Celata et al. [12] reviewed and resolved a number of heat transfer and fluid flow issues for the development and better understanding of microdevices.

Peng et al. [13, 14] performed an experimental investigation for a rectangular microchannel to analyze the effect of aspect ratio on forced-flow convection. It was concluded that the geometric parameters, especially the hydraulic parameter and aspect ratio, are important variables having a significant effect on the liquid flow through microchannels, and determined the frictional flow and heat transfer characteristics. Sobhan and Garimella [15] presented a comparative study of correlations for single-phase flow and heat transfer in microchannels proposed by various investigators. They discussed anomalies and deviations in the frictional and heat transfer characteristics from expected solutions for conventional sized channels. Steinke and Kandlikar [16] reviewed the available literature on single-phase liquid friction factors in microchannels. An in-depth comparison of previous experimental data was performed to identify the discrepancies in the reported literature. Pfahler et al. [17] argued that there is a critical dimension below which the general behavior of the experimental observations deviates from the N-S predictions.

Yu et al. [18] studied the fluid flow and heat transfer characteristics of nitrogen gas and water in micro-tubes. It was observed that the measured friction factors are slightly lower than the Moody chart values for both laminar and turbulent regimes. However, the Nusselt numbers in the turbulent regime are considerably higher than the predicted for conventional tubes. Adams et al. [19] investigated turbulent single-phase forced convection of water in circular microchannels. It was observed that the Nusselt numbers for the microchannels are higher than those predicted for traditional large channels.

Mala and Li [20] experimentally investigated the water flow through microtubes. The experimental results indicated that the friction factor is higher than compared to that predicted by the Poiseuille flow theory at high Reynolds number laminar flow condition. Lelea et al. [21] presented the experimental and numerical research on heat transfer and fluid flow in microchannel. It was concluded that the local value of $Nu$ is in good agreement with conventional theories including the entrance region. Yang et al. [22] experimentally investigated the pressure drop and heat transfer performance of air flow through microtubes with inside diameter of 86, 308 and 920 $\mu$m. The experimental results showed that the frictional coefficient of gas flow through a microtube is the same as that in the conventional larger tubes if the effect of gaseous flow compressibility was a well-taken consideration. Harms et al. [23] experimentally investigated the single-phase forced convection in a deep rectangular microchannel. It was observed that the experimentally obtained local Nusselt number agrees reasonably well with classical developing channel flow theory. Liu et al. [24, 25] numerically investigated the effect of variable fluid property on thermally developing flow in microchannel cooling passages. The flow and thermal redevelopment were observed due to the temperature-dependent viscosity and thermal conductivity. Such re-development leads to enhancement of the heat transfer near the channel wall.

Mahulikar and Herwig [26] reported the identification of laminar microconvection physical effects due to the variation of viscosity and thermal conductivity of the liquid. It was reported that a deviation in convection due to thermal conductivity variation exceeds the deviation due to viscosity variation, although the dimensionless viscosity-temperature sensitivity for water is higher than the dimensionless thermal conductivity-temperature sensitivity. Herwig and Mahulikar [27] investigated the effects of variable property in single-phase incompressible flows through microchannels. The deviations in Nusselt number from constant properties solution were observed due to variation in viscosity and thermal conductivity. Mahulikar et al. [28] reported a numerical simulation of pure continuum-based laminar gas microflow

convection with steep density gradients. Mahulikar and Herwig [29] numerically solved the governing continuum-based conservation equations for laminar 2D (with axisymmetry) convective microtube gas flow. It was indicated that the laminar microconvection characteristics are significantly affected due to physical effects induced by variations in gas properties. Gulhane and Mahulikar [30] investigated the influence of property variations of air in laminar forced convection with entrance effect. A significant deviation in Nusselt number from conventional theory was observed.

Gulhane and Mahulikar [31] numerically investigated the laminar microconvective liquid flow with entrance effect and Graetz problem due to variation in thermal properties. It was showed that the Nusselt number in the thermal entrance region deviates from constant properties solution due to scaling effects. Mahulikar and Herwig [32] re-examined the validity of Reynolds' analogy between Stanton number and the skin friction coefficient for microconvection of liquids with variations in fluid properties. The effects of property variations in single-phase laminar forced microconvection with CWHF BC were investigated by Gulhane and Mahulikar [33]. It was proposed that the deviation in convection with $c_{\mathrm{p}}(T)$, $k(T)$ variation is significant through temperature field than $\rho(p,T)$, $\mu(T)$ variation on velocity field. A numerical program was developed by Gulhane and Mahulikar [34] to solve 2D continuum-based governing differential equations for water flow in circular microchannel geometry. It was reported that the pressure drop significantly differs at the microscale compared to the macroscale. Nonino et al. [35, 36] and Giudice et al. [37] carried out a parametric investigation on the effects of temperature-dependent viscosity and viscous dissipation in simultaneously developing laminar flows of liquids in straight microchannels. It was confirmed that the temperature-dependent viscosity and viscous dissipation effects cannot be neglected in a wide range of operative conditions in the laminar forced convection in the entrance region of straight microchannels. Giudice et al. [38, 39] investigated the effects of temperature-dependent viscosity and thermal conductivity and of viscous dissipation on forced convection in simultaneously developing laminar flows of liquids in straight microchannels.

Kumar and Mahulikar [40] numerically investigated the effects of temperature-dependent viscosity variation on fully developed flow through a microchannel. Due to $\mu(T)$ variation, the concept of flow undevelopment was observed in the flow regime and the concept is valid throughout the transport phenomena. The frictional flow characteristics of water flowing through a circular microchannel with variable fluid properties were investigated by Kumar and Mahulikar [41].

### *1.1. Scope of Investigation*

The scope of the present work is to investigate the influence of property variations of water in laminar forced convection with entrance effect. The present work, by means of numerical results, examines the deviation in the heat transfer and fluid friction characteristics from constant property solution due to $\mu(T)$, $k(T)$ and combined $\mu(T)$ & $k(T)$ variations in water-microconvection. This study would be useful in better understanding of physics for incompressible fluid that provides an excellent performance of microdevices.

## 2. PROBLEM FORMULATION AND ANALYSIS

A circular cross section with an aspect ratio $(L/D) = 50$ is subjected to CWHF BC ($q''_{\mathrm{w}} > 0$, fluid heating) as shown schematically in Fig. 1. The physical mechanisms due to variations in properties are discussed for a hydrodynamically and thermally developing flow.

For all investigated cases, the following dimensions and input parameters are fixed: radius of microtube $R = 50 \times 10^{-6}$ m, length of microtube $L = 5 \times 10^{-3}$ m, inlet mean axial velocity $u_{\mathrm{m,in}} = 0.5$ m/s and inlet fluid temperature at the axis of microtube $T_{0,\mathrm{in}} = 293$ K. The values of aspect ratio, heat flux ($q''_{\mathrm{w}}$), inlet mean axial velocity ($u_{\mathrm{m,in}}$) and inlet fluid temperature on the axis of microtube ($T_{0,\mathrm{in}}$) are selected on the basis that the maximum temperature of water ($T_{\mathrm{w,ex}}$) in the computational domain should not exceed its boiling temperature.

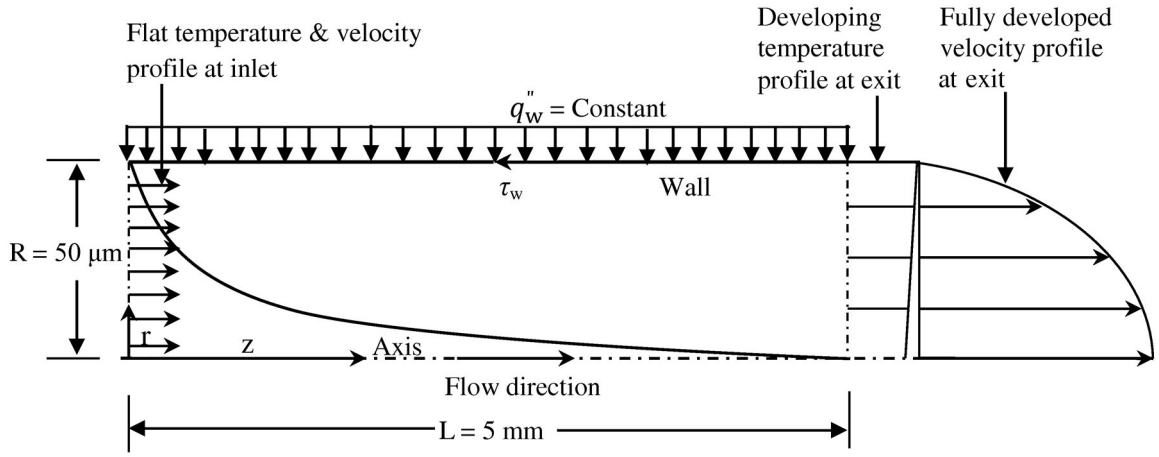


**Fig. 1.** A schematic of 2D (with axisymmetry) circular microchannel with CWHF boundary conditions.

### *2.1. Boundary Conditions*

Figure 1 is subjected to the following four thermal and flow boundary conditions:

1. Inlet: Flat velocity profile: $u(r,0) = u_{\text{in}}(r) = u_{\text{m,in}} = 0.5$ m/s and flat temperature profile: $T(r, 0) = T(r) = T_{0,\text{in}} = 293$ K. The subscript '0' refers to the value of parameter at the axis of microtube.

2. Outlet: $p_{\text{exit}} = 1.01325 \times 10^5$ Pa (atmospheric pressure) and $v_{\text{exit}} = 0$ since, $\partial u/\partial z = 0$.

3. Wall: The channel walls are nonporous rigid with $[k(\partial T/\partial r)]_{\text{w}} = q''_{\text{w}}$ and $u_{\text{w}}, v_{\text{w}} = 0$.

4. Axis: Symmetric boundary conditions are applied on the axis of microtube, hence, $(\partial u/\partial r) = (\partial T/\partial r) = (\partial p/\partial r) = (\partial \rho/\partial r) = 0$.

Inlet boundary condition reveals the role of fluid property variation mixing with entrance effects. From $z = 0^+$ (from inlet onwards) to $z = L$, the property variations for water are modeled as according to the cases, i.e., $\mu(T)$, $k(T)$, $\mu(T)$ & $k(T)$ variations. The flow is considered as Newtonian, laminar, single-phase, viscid, and non-isothermal. The effects of gravity, body forces, and radiation are ignored.

### *2.2. Mathematical Formulation*

The following steady state continuum-based, incompressible, laminar conservation governing equations (in nondimensional form) are numerically solved for water flowing through a microtube in an axisymmetric coordinate system, with $z$: axial coordinate, $r$: radial coordinate and $p$: pressure [32]. These four fluid flow and heat conservation equations have four unknowns ($u$, $v$, $p$, and $T$) also incorporate the additional physical effects due to $\mu(T)$ and $k(T)$ variations.

*Continuity equation*

$$(\bar{v}/\bar{r}) + (\partial \bar{v}/\partial \bar{r}) + (\partial \bar{u}/\partial \bar{z})/2 = 0. \tag{1}$$

*Momentum equation [axial direction]*

$$\begin{aligned} 2\bar{v} \cdot (\partial \bar{u}/\partial \bar{r}) + \bar{u} \cdot (\partial \bar{u}/\partial \bar{z}) &= -(\partial \bar{p}/\partial \bar{z})/2 + (2/Re_{\text{D}}) \cdot [(\bar{\mu}/\bar{r}) \\ +(\bar{S}_\mu \cdot \Pi_{S\mu}) \cdot (\partial\theta/\partial\bar{r})][2(\partial \bar{u}/\partial \bar{r}) + (\partial \bar{v}/\partial \bar{z})] &+ (2\bar{\mu}/Re_{\text{D}}) \cdot [(\partial^2 \bar{u}/\partial \bar{z}^2) \\ +2(\partial^2 \bar{u}/\partial \bar{r}^2) + (\partial^2 \bar{v}/\partial \bar{r} \cdot \partial \bar{z})] &+ (2\bar{S}_\mu/Re_{\text{D}}) \cdot \Pi_{\text{S}\mu} \cdot (\partial\theta/\partial\bar{z}) \cdot (\partial \bar{u}/\partial \bar{z}). \end{aligned} \tag{2}$$

Where, $\bar{p} = p/(\rho u_{\text{m}}^2/2)$, $\bar{\mu} = \mu/\mu_{\text{m}}$, $\bar{S}_\mu = S_\mu/S_{\mu m}$.

*Momentum equation [radial direction]*

$$2\bar{v}\cdot(\partial\bar{v}/\partial\bar{r})+\bar{u}\cdot(\partial\bar{v}/\partial\bar{z})=-(\partial\bar{p}/\partial\bar{r})+(8/Re_{\mathrm{D}})\cdot[(\bar{\mu}/\bar{r})$$

$$+(\bar{S}_{\mu}\cdot\Pi_{\mathrm{S}\mu})\cdot(\partial\theta/\partial\bar{r})](\partial\bar{v}/\partial\bar{r})+(\bar{\mu}/Re_{\mathrm{D}})\cdot[(\partial^2\bar{v}/\partial\bar{z}^2)-4(\bar{v}/\bar{r}^2) \tag{3}$$

$$+8(\partial^2\bar{v}/\partial\bar{r}^2)+2(\partial^2\bar{u}/\partial\bar{r}\cdot\partial\bar{z})]+(\bar{S}_{\mu}/Re_{\mathrm{D}})\cdot\Pi_{\mathrm{S}\mu}\cdot(\partial\theta/\partial\bar{z})[(\partial\bar{v}/\partial\bar{z})+2(\partial\bar{u}/\partial\bar{r})].$$

*Energy equation*

$$Pe_{\mathrm{D}}\cdot[(2\bar{v}\cdot(\partial\theta/\partial\bar{r})+\bar{u}\cdot(\partial\theta/\partial\bar{z})]=4[(\bar{k}/\bar{r})+(\bar{S}_{\mathrm{k}}\cdot\Pi_{\mathrm{Sk}})\cdot(k_{\mathrm{m}}/k_{\mathrm{m,in}})(\partial\theta/\partial\bar{r})](\partial\theta/\partial\bar{r})$$

$$+\bar{k}[4(\partial^2\theta/\partial\bar{r}^2)+(\partial^2\theta/\partial\bar{z}^2)]+(\Pi_{\mathrm{S_k}}\cdot\bar{S}_{\mathrm{k}})\cdot(k_{\mathrm{m}}/k_{\mathrm{m,in}})\cdot(\partial\theta/\partial\bar{z}^2), \tag{4}$$

where $\theta=k_{\mathrm{m,in}}\cdot(T-T_{\mathrm{m,in}})/(q''_{\mathrm{w}}\cdot D)$, $Pe_{\mathrm{D}}=Re_{\mathrm{D}}\cdot Pr$, $\bar{k}=k/k_{\mathrm{m}}$, and $\bar{S}_{\mathrm{k}}=S_{\mathrm{k}}/S_{\mathrm{km}}$.

The nondimensional parameters in governing equations (1)–(4) are as follows: $\bar{z}$ is the axial location ($=z/D$), $\bar{r}$ is the radial direction ($=r/R$), $\bar{u}$ is the axial velocity ($=u/u_{\mathrm{m}}$), $\bar{v}$ is the radial velocity ($=v/u_{\mathrm{m}}$), $\bar{\mu}$ is the viscosity ($=\mu/\mu_{\mathrm{m}}$), $\bar{k}$ is the thermal conductivity of water ($=k/k_{\mathrm{m}}$), $\bar{p}$ is the static pressure, $\theta$ is the temperature, $\bar{S}_{\mu}$ is the viscosity-temperature sensitivity, $\bar{S}_{\mathrm{k}}$ is the thermal conductivity-temperature sensitivity, $Pe_{\mathrm{D}}$ is the Peclet number based on $D$ ($=Re_{\mathrm{D}}\cdot Pr$). Mean value of the parameter is referred by subscript "m." The momentum and the energy equations are mutually coupled due to $\mu(T)$ variation in both radial and axial directions. In the nondimensional momentum equation, the modified nondimensional parameter $\Pi_{\mathrm{S}\mu}=|S_{\mu m}\cdot q''_{\mathrm{w}}\cdot D/(\mu_{\mathrm{m}}\cdot k_{\mathrm{m}})|$ and in nondimensional energy equation, the modified nondimensional parameter $\Pi_{\mathrm{S_k}}=|\mathrm{S_{km}}\cdot q''_{\mathrm{w}}\cdot D/(k^2_{\mathrm{m}})|$ are emerged. The $\Pi_{\mathrm{S}\mu}$ and $\Pi_{\mathrm{S_k}}$ are the magnitude of the product of the temperature perturbation parameter [$=f(q''_{\mathrm{w}}\cdot D/k)$] and nondimensional property sensitivities, $S_{\mu}(T/\mu)$ and $S_{\mathrm{k}}(T/\mu)$. The importance of momentum transport in the momentum equation is determined by $\mu(T)$ variation, which is shown by $\Pi_{\mathrm{S}\mu}$. The importance of momentum transport and energy flow due to fluid conduction is determined by $k(T)$ variation, which is shown by $\Pi_{\mathrm{Sk}}$. Higher value of $\Pi_{\mathrm{S}\mu}$ and $\Pi_{\mathrm{Sk}}$ is produced at large $q''_{\mathrm{w}}$, which shows the greater influence on microconvective flow due to variation in fluid properties [34].

### *2.3. Basic Equations Used in the Simulation*

The cross-sectionally averaged axial velocity is calculated as: $u_{\mathrm{m}}=(2/R^2)\int_0^R u(r)\cdot r\cdot dr$, and the enthalpy-averaged temperature of bulk fluid, which denotes the total energy of the flow at a particular location is defined as [31]: $T_{\mathrm{m}}=\int_0^R u(r)\cdot T(r)\cdot r\cdot dr/\int_0^R u(r)\cdot r\cdot dr$, for incompressible and constant $c_{\mathrm{p}}$ flow.

The Reynolds number ($Re$) is calculated as: $Re=\rho\cdot u_{\mathrm{m}}\cdot D/\mu_{\mathrm{m}}$. The Nusselt number ($Nu$) is defined as: $Nu=h\cdot D/k_{\mathrm{m}}$, where $h$ is the convective heat coefficient; $h=q''_{\mathrm{w}}/(T_{\mathrm{w}}-T_{\mathrm{m}})$ and the subscript "m" refers to the mean value of the properties calculated at $T_{\mathrm{m}}$. The $Nu$ can be written as: $Nu=q''_{\mathrm{w}}\cdot D/[(T_{\mathrm{w}}-T_{\mathrm{m}})\cdot k_{\mathrm{m}}]$. The Prandtl number ($Pr$) is defined as: $Pr=c_{\mathrm{p}}\cdot\mu_{\mathrm{m}}/k_{\mathrm{m}}$. The Fanning friction factor is defined as: $f_{\mathrm{F}}=\tau_{\mathrm{w}}/(\rho_{\mathrm{m}}\cdot u^2_{\mathrm{m}}/2)$, where $\tau_{\mathrm{w}}$ is the shear stress at the wall, $\tau_{\mathrm{w}}=\mu_{\mathrm{w}}\cdot(\partial u/\partial r)_{\mathrm{w}}$. The Darcy friction factor ($f_{\mathrm{D}}$) is equal to fourth times of $f_{\mathrm{F}}$; $f_{\mathrm{D}}=4f_{\mathrm{F}}$. The Poiseuille number ($Po$) is defined as the product of $f_{\mathrm{D}}$ and $Re$; $Po=f_{\mathrm{D}}\cdot Re$. For a fully developed flow with constant fluid properties, $Po=64$. The dimensionless wall velocity gradient is calculated as: $(\partial\bar{u}/\partial\bar{r})_{\mathrm{w}}=[(R/u_{\mathrm{m}})\cdot(\partial u/\partial r)_{\mathrm{w}}]$. The Peclet number ($Pe$) is equivalent to the product of the Reynolds number ($Re$) and the Prandtl number ($Pr$): $Pe=Re\cdot Pr$.

## 3. NUMERICAL METHOD AND VALIDATION

The fluid flow and heat conservation equations with boundary conditions are solved by the commercial CFD code, FLUENT. The pressure-based solver is used to achieve steady-state analysis for simulation. The SIMPLE (semi-implicit method for pressure-linked equations) scheme is selected for pressure-velocity coupling. The "standard" scheme is used for pressure interpolation and the second-order upwind scheme is used to discretize the convection terms in the momentum and energy equations. The energy equation is switched-on during the analysis to predict heat transfer effects in a microtube. The solution is considered converged when the plots of the residuals for continuity, $z$ and $r$ momentum, and energy equations are less than $10^{-15}$ or independent of the number of iterations.

A mesh is graded in order with the finer grid in the vicinity of the wall and the inlet to capture the abrupt change in flow and temperature fields. The graded mesh comprises 10000 cells [= 200 (in axial direction) × 50 (in radial direction)]. This grid system is conservatively selected on the basis of grid independence test of final results, i.e., $Po$ values. The accuracy of the numerical solution is checked by validating $Po$ results for a constant property solution. The results are confirmed with a benchmarked solution ($Po = 64$) and show a relative error lower than 0.06%. Additional details relating to the convergence of the solution, accuracy of the numerical results, and validation with benchmark cases for constant fluid properties are reported [26, 32, and 34].

### *3.1. Thermophysical Properties for Heat Transfer*

For water in the temperature range of 274–372 K, viscosity varies by 84%, thermal conductivity varies by 21%, density varies by 4%, and specific heat varies by 1% [42]. The $\mu(T)$ variation in kg/(m·s) for single-phase water is given by Sherman [43]:

$$\mu(T) = \mu(T_{\text{ref}}) \cdot (T/T_{\text{ref}})^n \cdot \exp[B(T^{-1} - T_{\text{ref}}^{-1})], \tag{5}$$

where $T$ is in K, $n = 8.9$, $B = 4700$, $\mu(T_{\text{ref}}) = 1.005 \times 10^{-3}$ kg/(m·s) at $T_{\text{ref}} = 293$ K.

The viscosity of water decreases with increasing temperature of water. The $k(T)$ variation in W/(m·K) for water is obtained as a least-square error third-order polynomial fitting of data in the working temperature range of 274–372 K. The $k(T)$ variation for single-phase water is given by cubic fit as [42]:

$$k(T) = 1.51721 + 0.0151476T - 3.5035 \times 10^{-5}T^2 + 2.74269 \times 10^{-8}T^3. \tag{6}$$

The thermal conductivity of water increases with increasing temperature of water. The variations in $\rho(T)$ and $c_{\text{p}}(T)$ are much less as compared to variations in $\mu(T)$ and $k(T)$, within the temperature range of 274–372 K; therefore, $\rho(T)$ and $c_{\text{p}}(T)$ variations are assumed to be constant [42]. The microconvective flow has the following characteristics: (1) Viscosity-temperature sensitivity ($S_{\mu T} = (\partial\mu/\partial T) < 0$) is negative since water viscosity decreases with increase in temperature. (2) Thermal conductivity-temperature sensitivity ($S_{\text{kT}} = (\partial k/\partial T) > 0$) is positive since water thermal conductivity increases with increase in temperature [31].

## 4. RESULTS AND DISCUSSION

### *4.1. Effects of Thermophysical Fluid Properties on the Local Nusselt Number*

The effects of temperature-dependent properties (viscosity and thermal conductivity) on the heat transfer are illustrated in this section. The local Nusselt numbers $Nu_{\mu(T)}$ for $\mu(T)$ variation, $Nu_{\text{k(T)}}$ for $k(T)$ variation, and $Nu_{\mu(T)\,\&\,k(T)}$ for combined $\mu(T)$ and $k(T)$ variations are calculated for different permissible heat fluxes, are compared with the corresponding local Nusselt number $Nu$ computed for constant property flows. Figure 2 illustrates the variation in $Nu_{\mu(T)}/Nu_{\text{CP}}$, $Nu_{k(T)}/Nu_{\text{CP}}$, and $Nu_{\mu(T)\,\&\,k(T)}/Nu_{\text{CP}}$ along the flow for different permissible heat fluxes. Figure 2a shows the effect of $\mu(T)$ variation ($\mu(T)$ variation alone is considered and $k$ is assumed constant = 0.6 W/(m·K)) on $Nu$ along the flow. The $\mu(T)$ variation indirectly affects the temperature field, because, the velocity field and temperature field are fully coupled with each other due to $\mu(T)$ variation. The radially inward flow due

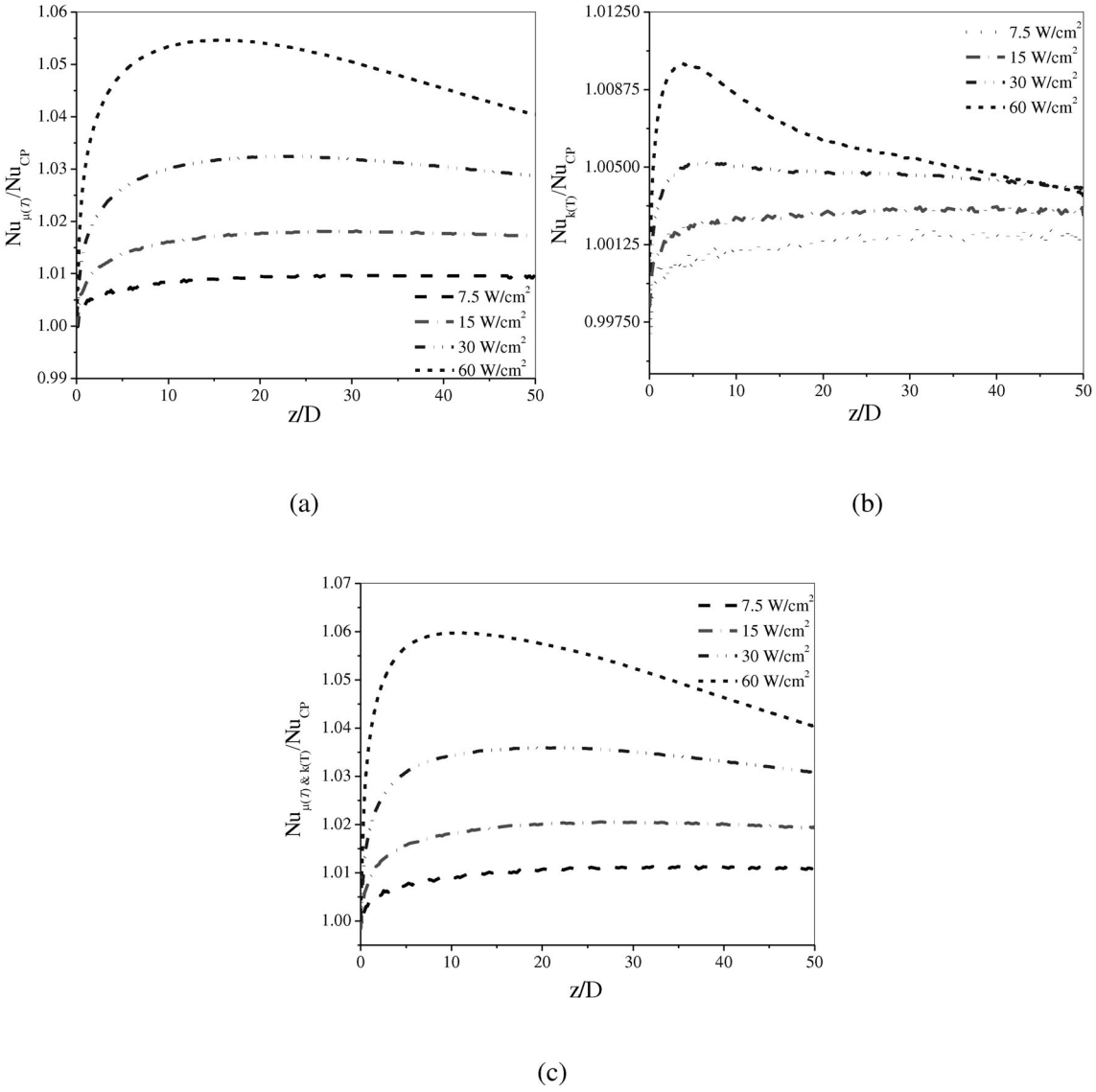


**Fig. 2.** The effect of wall heat flux on the variation of $Nu_{\mathrm{VP}}/Nu_{\mathrm{CP}}$ along the flow: (a) $\mu(T)$ variation; (b) $k(T)$ variation; (c) $\mu(T)$ & $k$(T) variation.

to hydrodynamic development is alleviated due to the counter effect of induced radially outward flow due to $\mu(T)$ variation. Hence, the $Nu$ decrease rate is alleviated for the case of water heated, therefore, $Nu_{\mu(T)}/Nu_{\mathrm{CP}} > 1$. It is observed that the $\mu(T)$ variation improves convection due to faster moving particles closer to the wall. The temperature near the wall is higher as compared to the centerline of the tube due to constant heat supplied from the wall. Therefore, the higher viscosity fluid exists on the centerline of the tube, which reduces the axial velocity on the centerline. This is called a flattening effect, which induces radially outward undeveloped flow due to $\mu(T)$ variation [34]. However, the lower viscosity fluid exists close to the wall, which provides a larger mass flux (due to a higher velocity fluid close to the wall) close to the wall, thereby enhancing convection performance. The convective heat transfer is significantly affected by non-negligible outward radial flow and radial convection because $Nu \propto (\partial u/\partial r)_{\mathrm{w}}$ [34]. The variation in $[(\partial \bar{u}/\partial \bar{r})_{\mathrm{w}}]_{\mu(T)}/[(\partial \bar{u}/\partial \bar{r})_{\mathrm{w}}]_{\mathrm{CP}}$ along the flow is shown in Fig. 3. It is observed that, firstly, the $Nu$ for the $\mu(T)$ variation increases along the flow due to the flattening of the axial velocity profile and then it decays due to the slight sharpening of the axial velocity profile along the flow [26]. It is noted that the $Nu$ for the $\mu(T)$ variation increases with increase in the wall heat flux.

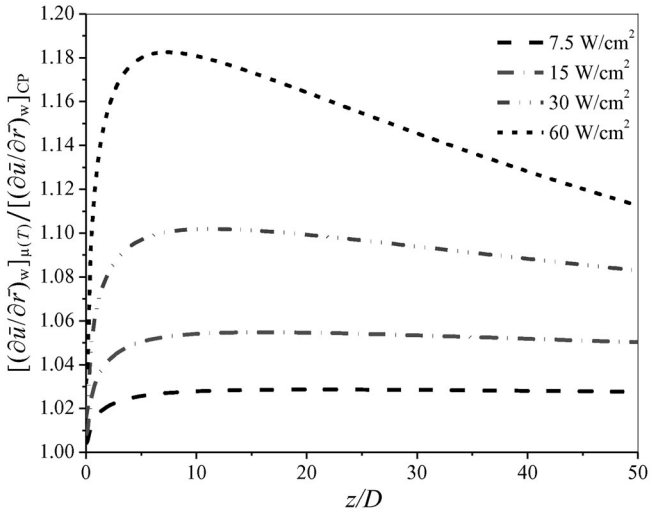


**Fig. 3.** The effect of wall heat flux on the variation of $[(\partial\bar{u}/\partial\bar{r})_{\rm w}]_{\mu(T)}/[(\partial\bar{u}/\partial\bar{r})_{\rm w}]_{\rm CP}$ along the flow for $\mu(T)$ variation.

$h_{\rm VP}/h_{\rm CP}$ and $Nu_{\rm VP}/Nu_{\rm CP}$-variations considering $\mu(T)$ variation only, $k(T)$ variation only, combined $\mu(T)$ & $k(T)$ variations

| $q''_{\rm w}$ (W/cm$^2$) | $[h_{\mu(T)}/h_{\rm CP}]_{\rm max}$ | $[h_{k(T)}/h_{\rm CP}]_{\rm max}$ | $[h_{\mu(T)\&k(T)}/h_{\rm CP}]_{\rm max}$ | $[Nu_{\mu(T)}/Nu_{\rm CP}]_{\rm max}$ | $[Nu_{k(T)}/Nu_{\rm CP}]_{\rm max}$ | $[Nu_{\mu(T)\&k(T)}/Nu_{\rm CP}]_{\rm max}$ |
|---|---|---|---|---|---|---|
| 7.5 | 1.0097 | 1.0263 | 1.0360 | 1.0097 | 1.0020 | 1.0114 |
| 15 | 1.0182 | 1.0451 | 1.0623 | 1.0182 | 1.0031 | 1.0205 |
| 30 | 1.0324 | 1.0763 | 1.1051 | 1.0324 | 1.0052 | 1.0359 |
| 60 | 1.0546 | 1.1193 | 1.1602 | 1.0546 | 1.0100 | 1.0597 |

Figure 2b shows the effect of $k(T)$ variation (the $k(T)$ variation alone is considered and $\mu$ is assumed constant $= 1.005 \times 10^{-3}$ kg/(m·s)) on $Nu$ along the flow. The heat flow at the cross section is given by $q''_{\rm w} = k_{\rm w} \cdot (\partial T/\partial r)_{\rm w}$. For constant heat flux supplied from the wall ($q''_{\rm w}$), the $k_{\rm w}$ increases along the flow, which reduces the corresponding temperature gradient near the wall $(\partial T/\partial r)_{\rm w}$ and reduces the wall temperature ($T_{\rm w}$). The $k(T)$ variation directly affects the temperature field by flattening the radial temperature profile; thus, a "U"-shaped $k(r)$ profile enhances convection compared to $Nu_{\rm CP}$ [31]. The thermal conductivity variation across the flow leads to higher $Nu$ for the case of water heated, because higher thermal conductivity fluid exists near the wall due to higher temperature near the wall (due to constant heat supplied from the wall). The higher thermal conductivity fluid near the wall is more effective in convecting away the imposed thermal boundary condition at the wall compared to the higher thermal conductivity fluid near the centerline of the microtube [26]. It is noted that the $Nu$ for $k(T)$ variation significantly deviates from $Nu_{\rm CP}$. For same wall heat flux, this deviation is less than as compared to the case of $\mu(T)$ variation. Although, the variation in the convective heat transfer coefficient ($h$) for the $k(T)$ variation is higher than that of the $\mu(T)$ variation as shown in Fig. 4. The reason behind this is: the $k_{\rm m}$ continuously increases along the flow for the $k(T)$ variation, which reduces the deviation in $Nu$ from constant property solution. However, the $k_{\rm m}$ is constant along the flow for $\mu(T)$ variation. The deviation in $Nu$ from $Nu_{\rm CP}$ increases with increase in the wall heat flux for $k(T)$ variation.

Figure 2c shows the effect of combined $\mu(T)$ and $k(T)$ variations on the $Nu$ along the flow. It is noted that the deviation in the $Nu$ for combined $\mu(T)$ and $k(T)$ variations from $Nu_{\rm CP}$ is higher than that of $\mu(T)$ variation as shown in Fig. 5. The incorporation of $k(T)$ variation with $\mu(T)$ variation increases

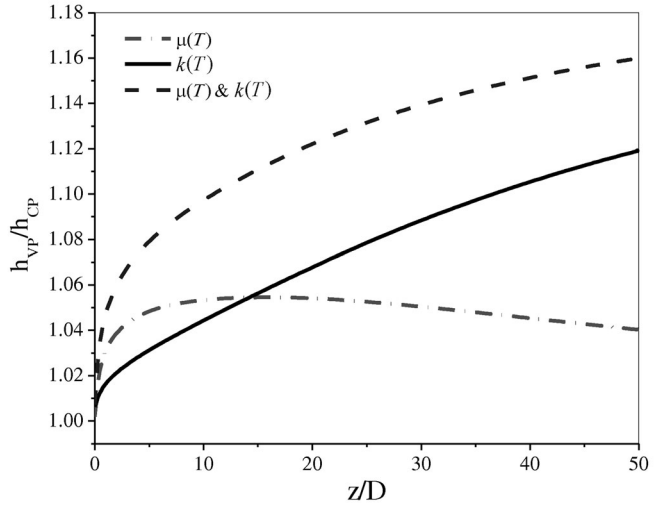


**Fig. 4.** The effect of fluid property variation on $h_{\mathrm{VP}}/h_{\mathrm{CP}}$ along the flow for $q''_{\mathrm{w}} = 60\ \mathrm{W/cm^2}$.

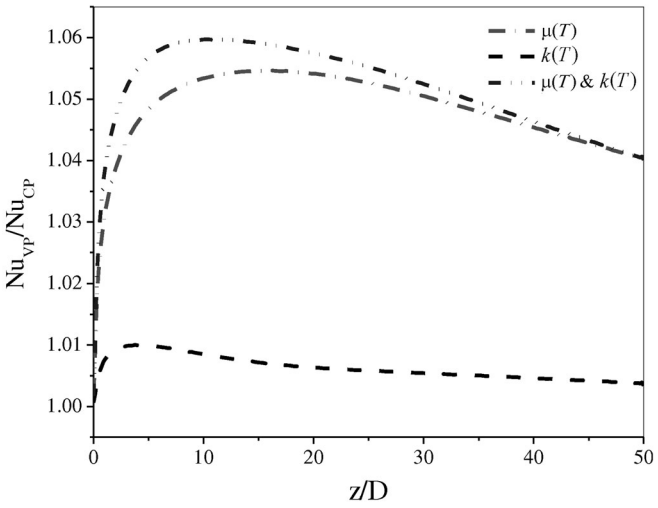


**Fig. 5.** The effect of fluid property variation on $Nu_{\mathrm{VP}}/Nu_{\mathrm{CP}}$ along the flow for $q''_{\mathrm{w}} = 60\ \mathrm{W/cm^2}$.

the $Nu$ along the flow. The values of $[Nu_{\mathrm{VP}}/Nu_{\mathrm{CP}}]_{\max}$ for the three cases are given in the table, which illustrates popular belief of the asymptotic theory as [2]:

$$[Nu_{\mu(T)\,\&\,k(T)}/Nu_{\mathrm{CP}}] > [Nu_{\mu(T)}/Nu_{\mathrm{CP}}] > [Nu_{\mathrm{k(T)}}/Nu_{\mathrm{CP}}].$$

The augmentation in the convective heat transfer coefficient is highest for combined $\mu(T)$ and $k(T)$ variations and the augmentation in the convective heat transfer coefficient is lowest for $\mu(T)$ variation as illustrated in Fig. 4 and given in the table. Figure 4 shows the following order of $h_{\mathrm{VP}}/h_{\mathrm{CP}}$:

$$[h_{\mu(T)\,\&\,k(T)}/h_{\mathrm{CP}}] > [h_{k(T)}/h_{\mathrm{CP}}] > [h_{\mu(T)}/h_{\mathrm{CP}}].$$

The augmentation in the convective heat transfer coefficient for the $k(T)$ variation is large as compared to the $\mu(T)$ variation, although the dimensionless temperature sensitivity of viscosity is higher than that of thermal conductivity.

### *4.2. Effects of Temperature-Dependent Properties on the $f_F$, Po, Pr, Pe*

The effects of temperature-dependent properties (viscosity and thermal conductivity) on fanning friction factor ($f_F$) are illustrated in Fig. 6. Figure 6a illustrates the effect of $\mu(T)$ variation on $f_F$. The $\mu(T)$ variation directly affects the velocity field due to flattening of the $u(r,z)$ profile. The $\mu(T)$ variation plays an important role in determining the flow resistance because viscosity temperature sensitivity is much higher for water. The role of the $\mu(T)$ variation on the $\tau_w$ is explained as follows [34]: $d\tau_w/dz = \mu_w \cdot \partial/\partial z(\partial u/\partial r)_w + (\partial u/\partial r)_w \cdot (\partial \mu_w/\partial z)$, because $\tau_w = \mu_w \cdot (\partial u/\partial r)_w$. The value of $(f_{F,\mu(T)}/f_{F,CP})$ continuously decreases along the flow due to the continuous reduction in viscosity with increasing temperature, which reduces friction along the flow as $(\partial \mu_w/\partial z) > 0$. It is observed that the value of $(f_{F,\mu(T)}/f_{F,CP})$ decreases with an increase in the wall heat flux. Figure 6b illustrates the effect of the $k(T)$ variation on the $f_F$. It is observed that the $k(T)$ variation is not able to produce any effect on the $f_F$, therefore, the value of $(f_{F,k(T)}/f_{F,CP})$ is equal to 1. The main reason behind this is: when the $k(T)$ variation alone is considered, the velocity field is independent of the temperature field. The value of $(f_{F,k(T)}/f_{F,CP})$ is equal to 1 for each wall heat flux. Figure 6c illustrates the effect of combined $\mu(T)$ and $k(T)$ variations on the $f_F$. When $\mu(T)$ and $k(T)$ variations are incorporated, the fluid velocity field

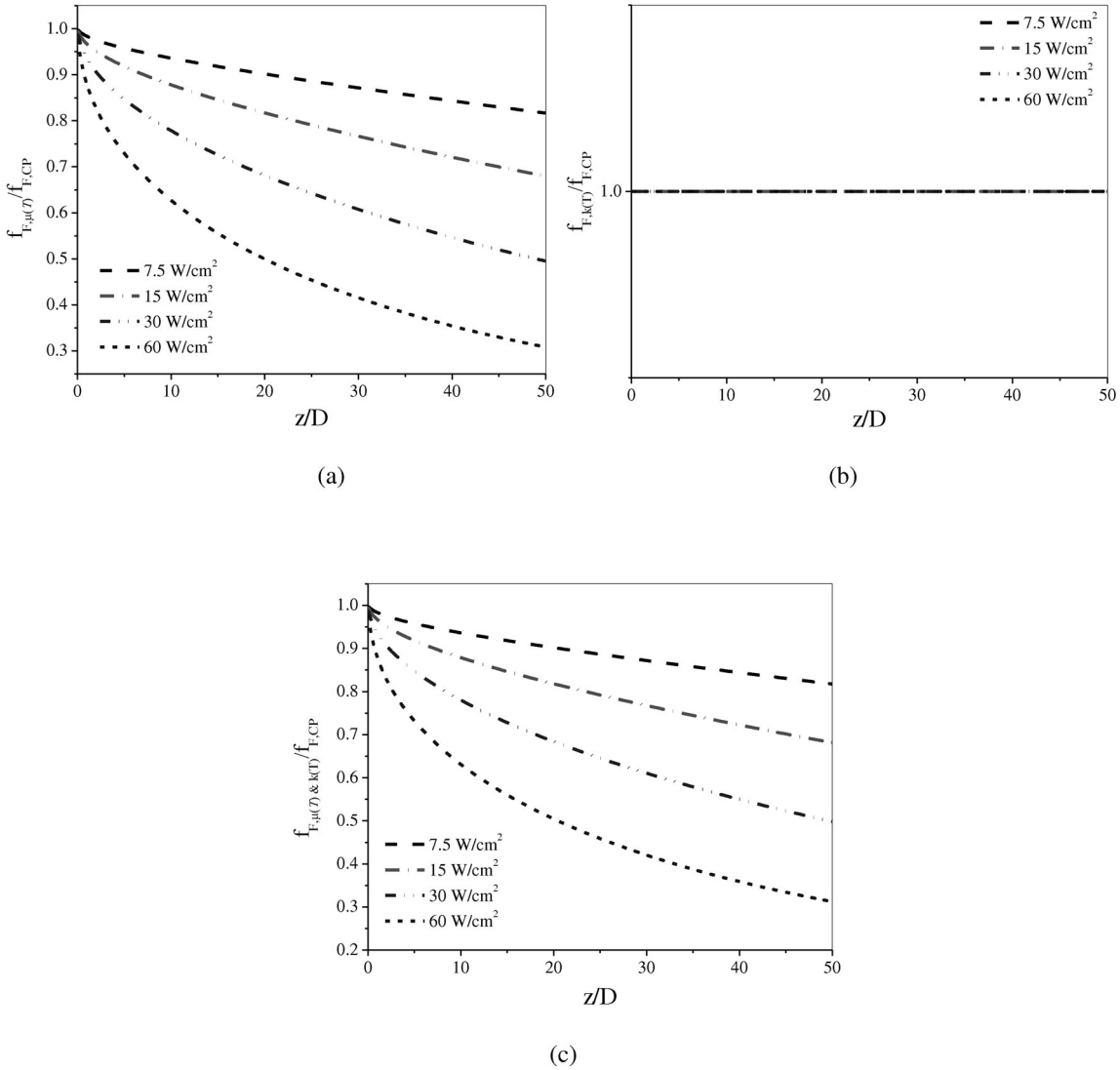


**Fig. 6.** The effect of wall heat flux on the variation of $f_{F,VP}/f_{F,CP}$ along the flow: (a) $\mu(T)$ variation; (b) $k(T)$ variation; (c) $\mu(T)$ & $k(T)$ variation.

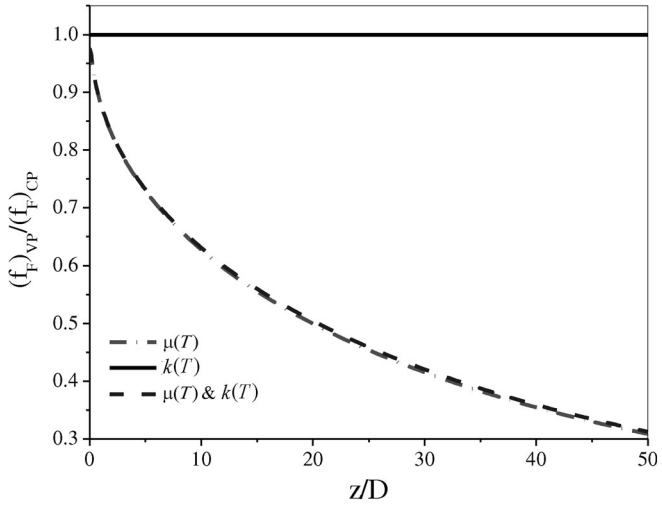


**Fig. 7.** The effect of fluid property variation on $f_{\mathrm{VP}}/f_{\mathrm{CP}}$ along the flow for $q''_{\mathrm{w}} = 60\ \mathrm{W/cm^2}$.

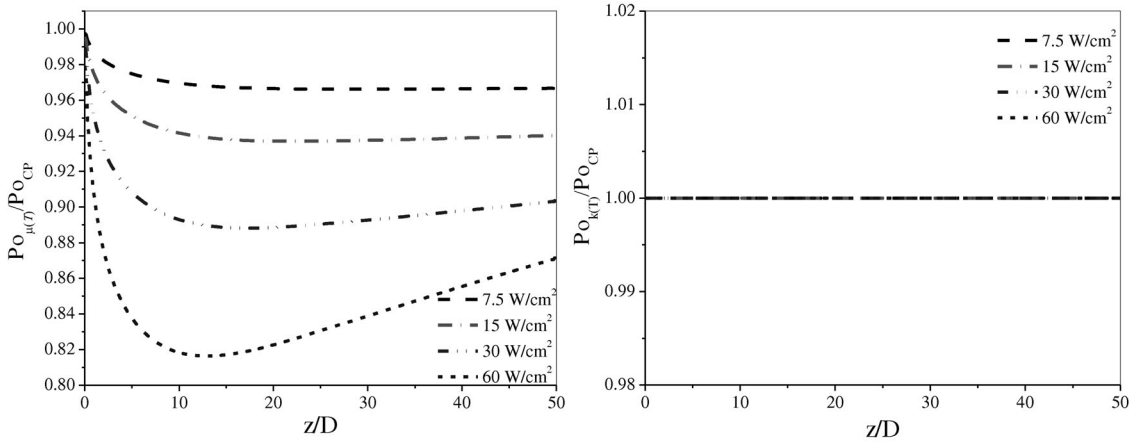


(a) (b)

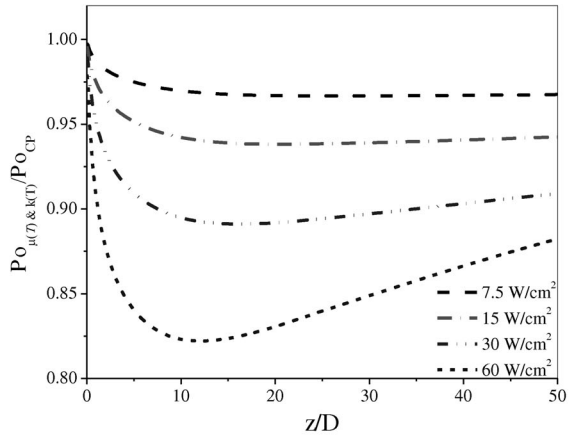


(c)

**Fig. 8.** The effect of wall heat flux on the variation of $Po_{\mathrm{VP}}/Po_{\mathrm{CP}}$ along the flow: (a) $\mu(T)$ variation; (b) $k(T)$ variation; (c) $\mu(T)$ & $k$(T) variation.

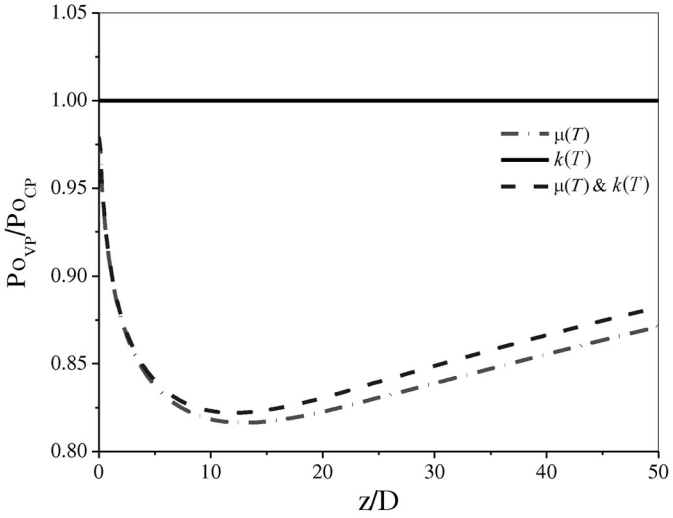


**Fig. 9.** The effect of fluid property variation on $Po_{\mathrm{VP}}/Po_{\mathrm{CP}}$ along the flow for $q''_{\mathrm{w}} = 60\ \mathrm{W/cm^2}$.

is highly coupled with the temperature field, and the momentum equation is no longer independent of the energy equation. Therefore, the incorporation of $k(T)$ variation with $\mu(T)$ variation leads to a slight increment in friction as shown in Fig. 7. Incorporating the $k(T)$ variation reduces wall temperature and alleviates the temperature gradient, thereby increasing the friction [34].

The Poiseuille number ($Po$) deviates from the constant properties solution due to the $\mu(T)$ variation, as illustrated in Fig. 8a. Firstly, $Po_{\mu(T)}/Po_{\mathrm{CP}}$ decreases rapidly and attains its minimum value, and after that, it increases along the flow. The reason behind this is: the rate of reduction in $f_{\mathrm{F}}$ is higher as compared to the increment in $Re$ in the entrance region, thereby $Po_{\mu(T)}/Po_{\mathrm{CP}}$ decreases rapidly in the entrance region. However, after the entrance region, the rate of reduction in $f_{\mathrm{F}}$ is lower as compared to the increment in $Re$, thereby $Po_{\mu(T)}/Po_{\mathrm{CP}}$ increases along the flow. The deviation in $Po_{\mu(T)}$ from $Po_{\mathrm{CP}}$ increases with an increase in the wall heat flux. The $k(T)$ variation is not able to produce any effect on $Po$ as illustrated in Fig. 8b. Figure 8c shows the effect of combined $\mu(T)$ and $k(T)$ variations on $Po$. The value of $Po_{\mu(T)\,\&\,k(T)}/Po_{\mathrm{CP}}$ decreases with an increase in wall heat flux. The incorporation of $k(T)$ variation with $\mu(T)$ variation leads to an increase in the $Po_{\mu(T)\,\&\,k(T)}/Po_{\mathrm{CP}}$, as shown in Fig. 9. This increment is due to slight increment in $f_{\mathrm{F}}$ as illustrated in Fig. 7.

The effects of property variation on the Prandtl number ($Pr$) are illustrated in Fig. 10. The $Pr \cong 7$, for constant fluid properties. The $\mu(T)$ variation leads to a decrease in the $Pr$ along the flow as shown in Fig. 10a. The $\mu_{\mathrm{m}}$ decreases along the flow due to $S_{\mu T} < 0$, $c_{\mathrm{p}}$ and $k$ is constant for the $\mu(T)$ variation flow. Therefore, the $Pr$ decreases along the flow. The rate of reduction in the $Pr$ increases with an increase in the wall heat flux. The $k(T)$ variation leads to a decrease in the $Pr$ along the flow as shown in Fig. 10b. The $k_{\mathrm{m}}$ increases along the flow due to $S_{\mathrm{kT}} > 0$, $c_{\mathrm{p}}$ and $\mu$ is constant for the $k(T)$ variation flow. For same wall heat flux, the rate of reduction in the $Pr$ is lower for the $k(T)$ variation as compared to the $\mu(T)$ variation due to high viscosity-temperature sensitivity, as shown in Fig. 11. The effect of combined $\mu(T)$ and $k(T)$ variations on the $Pr$ is illustrated in Fig. 10c. The role of combined $\mu(T)$ and $k(T)$ variations is to reduce the $Pr$ along the flow. The $\mu_{\mathrm{m}}$ decreases along the flow due to $S_{\mu T} < 0$, the $k_{\mathrm{m}}$ increases along the flow due to $S_{\mathrm{kT}} > 0$, and $c_{\mathrm{p}}$ is constant, therefore, the rate of reduction in the $Pr$ is higher for combined $\mu(T)$ and $k(T)$ variations as compared to the $\mu(T)$ variation as shown in Fig. 11.

The variations in the Peclet number ($Pe$) along the flow for different thermophysical properties are illustrated in Fig. 12. The $\mu(T)$ variation is not able to produce any effect on $Pe$ as illustrated in Fig. 12a. This is because: $Pe = Re \cdot Pr = (\rho \cdot u_{\mathrm{m}} \cdot D/\mu_{\mathrm{m}}) \cdot (\mu_{\mathrm{m}} \cdot c_{\mathrm{p}}/k_{\mathrm{m}}) = (\rho \cdot u_{\mathrm{m}} \cdot D \cdot c_{\mathrm{p}}/k_{\mathrm{m}})$ does not depend on $\mu_{\mathrm{m}}$. Therefore, the value of $Pe_{\mu(T)}/Pe_{\mathrm{CP}} = 1$. For the $k(T)$ variation, the $k_{\mathrm{m}}$ increases along the flow, therefore the $k(T)$ variation leads to reducing $Pe$, as shown in Fig. 12b. The effect of combined $\mu(T)$ and $k(T)$ variations on the $Pe$ is illustrated in Fig. 12c. The incorporation of the $\mu(T)$ variation with the

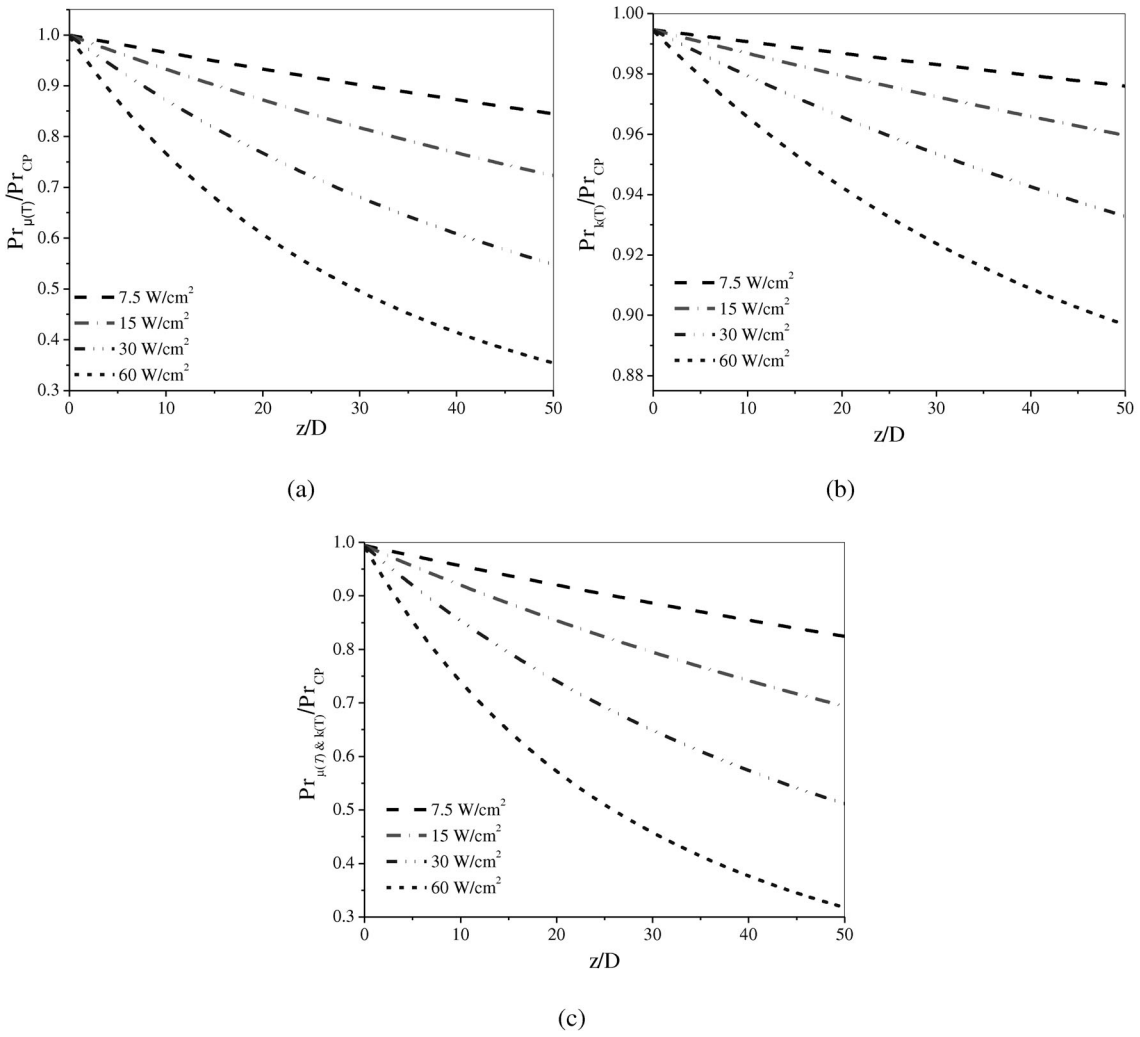


**Fig. 10.** The effect of wall heat flux on the variation of $Pr_{\mathrm{VP}}/Pr_{\mathrm{CP}}$ along the flow: (a) $\mu(T)$ variation; (b) $k(T)$ variation; (c) $\mu(T)$ & $k$(T) variation.

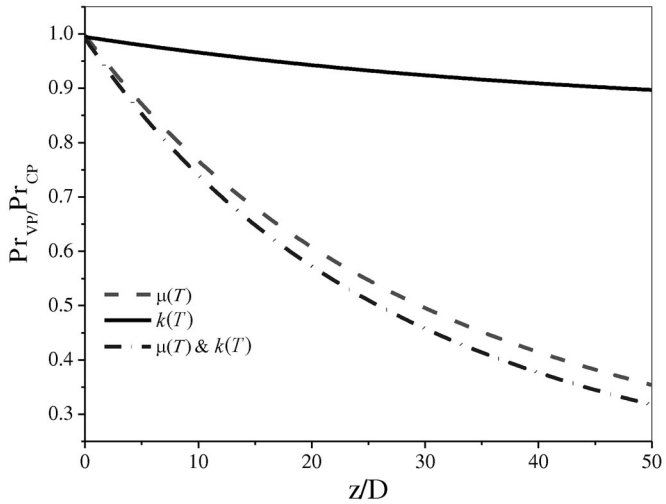


**Fig. 11.** The effect of fluid property variation on $Pr_{\mathrm{VP}}/Pr_{\mathrm{CP}}$ along the flow for $q''_{\mathrm{w}} = 60\ \mathrm{W/cm^2}$.

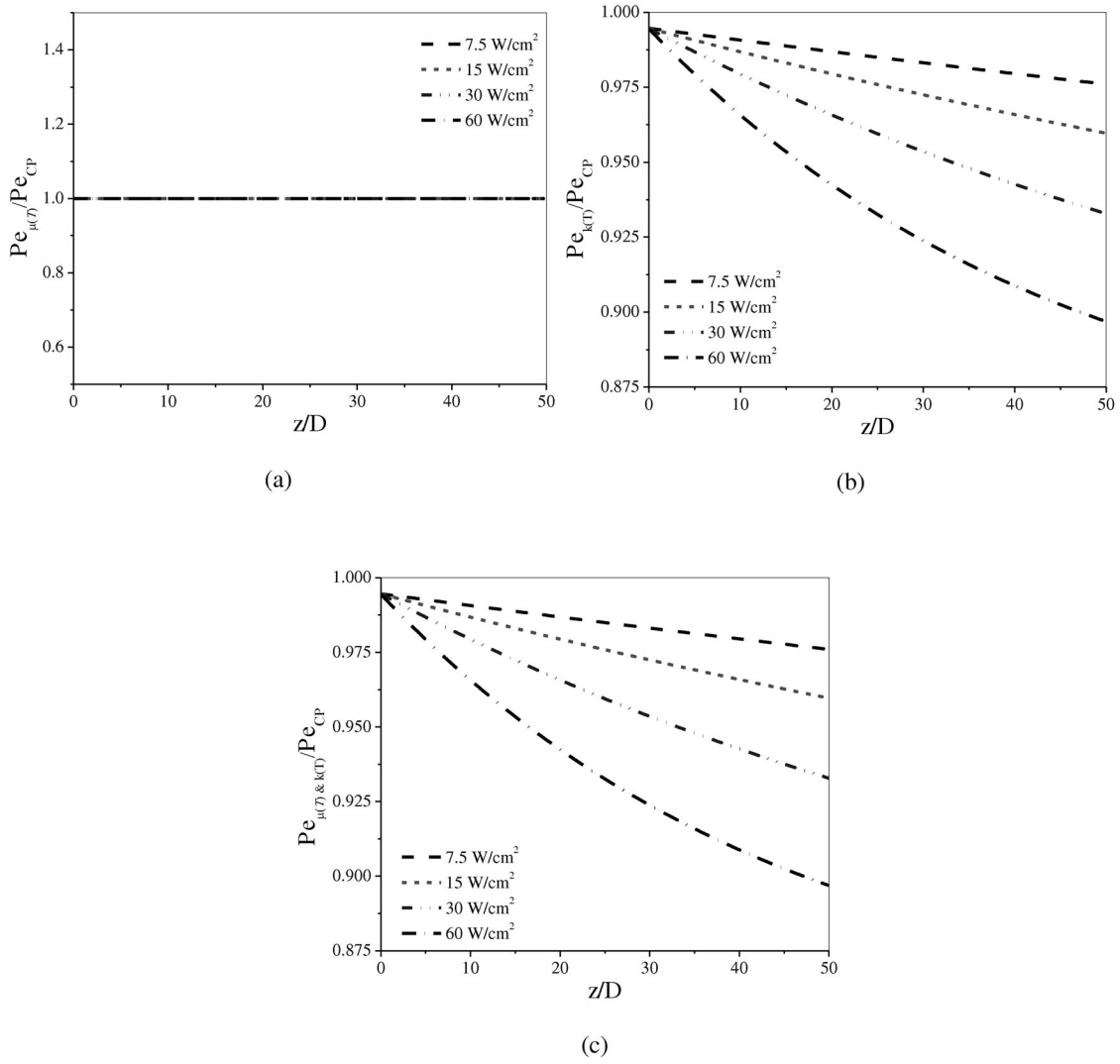


**Fig. 12.** The effect of wall heat flux on the variation of $Pe_{\mathrm{VP}}/Pe_{\mathrm{CP}}$ along the flow: (a) $\mu(T)$ variation; (b) $k(T)$ variation; (c) $\mu(T)$ & $k$(T) variation.

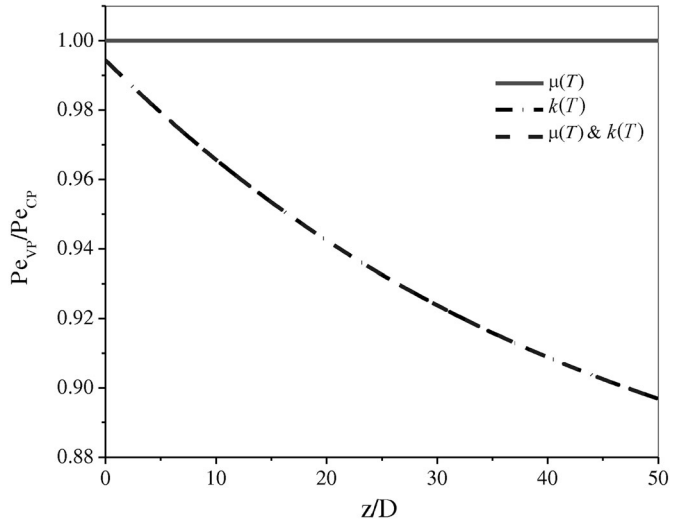


**Fig. 13.** The effect of fluid property variation on $Pe_{\mathrm{VP}}/Pe_{\mathrm{CP}}$ along the flow for $q''_{\mathrm{w}} = 60\ \mathrm{W/cm^2}$.

$k(T)$ variation is not able to produce any effect on the $Pe$ as illustrated in Fig. 13. The main effects of temperature-dependent fluid properties on the $Pe$ can be retained even if only thermal conductivity is allowed to vary with temperature while the viscosity is assumed constant. It can be verified as:

$$Pe_{\mu(T)\,\&\,k(T)}/Pe_{\mathrm{CP}} = (Pe_{\mu(T),k(T)} \cdot Pe_{k(T)})/(Pe_{k(T)} \cdot Pe_{\mathrm{CP}}).$$

From Fig. 13, $(Pe_{\mu(T)\,\&\,k(T)} \cdot Pe_{k(T)}) = 1$, therefore $(Pe_{\mu(T)\,\&\,k(T)}/Pe_{\mathrm{CP}}) = (Pe_{k(T)} \cdot Pe_{\mathrm{CP}})$.

Therefore, the variations in $Pe_{\mu(T)\,\&\,k(T)}/Pe_{\mathrm{CP}}$ and $(Pe_{k(T)} \cdot Pe_{\mathrm{CP}})$ along the flow coincide on the same line as shown in Fig. 13.

## 5. CONCLUSIONS

The effects of temperature-dependent viscosity and thermal conductivity on heat transfer and frictional flow characteristics of hydrodynamically and thermally developing flow of liquid in the entrance region with a no-slip, no-temperature jump boundary condition were numerically studied in this paper. The 2D continuum-based conservation equations for microconvective flow were numerically solved and the following observations were noted:

1. The obtained $Nu$ shows a significant deviation from conventional theory due to flattening of axial velocity profile due to $\mu(T)$ variation. The $\mu(T)$ variation improves convection due to faster moving particles closer to the wall. Therefore, the $Nu$ decrease rate is alleviated for the case of water heated, hence, $Nu_{\mu(T)}/Nu_{\mathrm{CP}} > 1$. The value of $(f_{\mathrm{F},\mu(\mathrm{T})}/f_{\mathrm{F,CP}})$ continuously decreases along the flow due to the continuous reduction in viscosity with increasing temperature.

2. The obtained $Nu$ shows a significant deviation from conventional theory due to flattening of the radial temperature profile due to the $k(T)$ variation, which reduces the wall temperature gradient. The thermal conductivity variation across the flow leads to higher $Nu$ for the case of water heated, because higher thermal conductivity fluid exists near the wall, therefore, $Nu_{k(T)}/Nu_{\mathrm{CP}} > 1$. The $k(T)$ variation does not produce any effect on the Fanning friction factor.

3. The rate of decrease in $Nu$ for combined $\mu(T)$ and $k(T)$ variations is lower as compared to the $\mu(T)$ variation, therefore the deviation in the $Nu_{\mu(T)\,\&\,k(T)}/Nu_{\mathrm{CP}}$ is maximum. It is observed that the incorporation of $k(T)$ variation with $\mu(T)$ variation leads to a slight increment in the Fanning friction factor.

4. The $\mu(T)$ variation leads to a decrease in $Pr$ along the flow. However, for same wall heat flux, the rate of reduction in the $Pr$ is lower for the $k(T)$ variation as compared to the $\mu(T)$ variation due to high viscosity-temperature sensitivity. The rate of reduction in $Pr$ is higher for combined $\mu(T)$ and $k(T)$ variations as compared to the $\mu(T)$ variation.

5. It is noted that the main effects of temperature-dependent fluid properties on the Peclet number can be retained even if only thermal conductivity is allowed to vary with temperature while the viscosity is assumed constant.

6. The above results indicate that the variations in fluid properties need to be properly accounted in microconvection applications and the flow cannot be simply considered a constant properties flow as in conventional thermal designs.

## ACKNOWLEDGMENTS

The authors thank the seed grant research project no. IITM/SG/SPM/28 of Indian Institute of Technology (IIT) Mandi, Himachal Pradesh. The authors are grateful to IIT Bombay for granting deputation (in public interest) to Prof. Shripad P. Mahulikar at IIT Mandi from June 1, 2013 to December 31, 2014, vide office Order no. Admn-I/246/2013. The authors would like to thank Dr. Syed Abbas, Assistant Professor, School of Basic Sciences, IIT Mandi, India, for the administrative support.

## NOTATIONS

$D$—diameter of microtube [m]

$L$—length of microtube [m]

$h$—heat transfer coefficient [$\mathrm{W{\cdot}m^{-2}{\cdot}K^{-1}}$]

$q''_{\mathrm{w}}$—heat flux at the wall [$\mathrm{W{\cdot}m^{-2}}$]

$T_0$—inlet temperature [K]

$T_{\mathrm{m}}$—bulk mean temperature [K]

$T_{\mathrm{w}}$—wall temperature [K]

$(\partial u/\partial r)_{\mathrm{w}}$—wall velocity gradient [$\mathrm{s^{-1}}$]

### *Greek Symbols*

$\rho(T)$—temperature-dependent density [$\mathrm{kg{\cdot}m^{-3}}$]

$c_{\mathrm{p}}(T)$—temperature-dependent specific heat at constant pressure [$\mathrm{J{\cdot}kg^{-1}{\cdot}K^{-1}}$]

$k(T)$—temperature-dependent thermal conductivity [$\mathrm{W{\cdot}m^{-1}{\cdot}K^{-1}}$]

$\mu(T)$—temperature-dependent viscosity [$\mathrm{N{\cdot}s{\cdot}m^{-2}}$]

$\tau_{\mathrm{w}}$—shear stress at the wall [$\mathrm{N{\cdot}m^{-2}}$]

$S_{\mathrm{k}}$—thermal conductivity temperature sensitivity $(\partial k/\partial T)$

$S_{\mu}$—viscosity temperature sensitivity $(\partial \mu/\partial T)$

### *Non-Dimensional Numbers*

$Nu$—Nusselt number $(h \cdot D/k_{\mathrm{m}})$

$Pe$—Peclet number $(\rho_{\mathrm{m}} \cdot u_{\mathrm{m}} \cdot c_{\mathrm{p}} \cdot D/k_{\mathrm{m}})$

$Po$—Poiseuille number $(f \cdot Re_{\mathrm{D}})$

$Pr$—Prandtl numbers $(c_{\mathrm{p}} \cdot \mu_{\mathrm{m}}/k_{\mathrm{m}})$

$Re$—Reynolds number $(\rho_{\mathrm{m}} \cdot u_{\mathrm{m}} \cdot D/\mu_{\mathrm{m}})$

### *Subscripts*

CP—constant properties

D—based on the diameter

ex—value at the outlet

in—value at the inlet

m—mean value of properties calculated at bulk mean temperature, $T_{\mathrm{m}}$

VP—variable properties

w—condition at the wall

## REFERENCES


1. Shah, R.K. and London, A.L., *Laminar Flow Forced Convection in Ducts: A Source Book for Compact Heat Exchanger Analytical Data*, New York: Academic Press, 1978.
2. Herwig, H., The Effect of Variable Properties on Momentum and Heat Transfer in a Tube with Constant Heat Flux across the Wall, *Int. J. Heat Mass Transfer*, 1985, vol. 28, pp. 423–431.
3. Herwig, H., Voigt, M., and Bauhaus, F.J., The Effect of Variable Properties on Momentum and Heat Transfer in a Tube with Constant Wall Temperature, *Int. J. Heat Mass Transfer*, 1989, vol. 32, pp. 1907–1915.
4. Sieder, E.N. and Tate, C.E., Heat Transfer and Pressure Drop of Liquids in Tubes, *Ind. Eng. Chem.*, 1936, vol. 28, pp. 1429–1433.
5. Kakac, S., Shah, R.K., and Aung, W., *Handbook of Single-Phase Convective Heat Transfer*, New York: Wiley, 1987.
6. Tunc, G. and Bayazitoglu, Y., Heat Transfer in Rectangular Microchannels, *Int. J. Heat Mass Transfer*, 2002, vol. 45, pp. 765–773.
7. Tunc, G. and Bayazitoglu, Y., Heat Transfer in Microtube with Viscous Dissipation, *Int. J. Heat Mass Transfer*, 2001, vol. 44, pp. 2395–2403
8. Palm, B., Heat Transfer in Microchannels, *Microscale Therm. Eng.*, 2001, vol. 5, pp. 155–175.
9. Mahulikar, S.P., Herwig, H., and Hausner, O., Study of Gas Microconvection for Synthesis of Rarefaction and Nonrarefaction Effects, *IEEE/ASME J. Microelectromech. Syst.*, 2007, vol. 16, pp. 1543–1556.
10. Ameel, T.A., Wang, X.M., Barron, R.F., and Warrington, R.O., Laminar Forced Convection in a Circular Tube with Constant Heat Flux and Slip Flow, *Microscale Therm. Eng.*, 1997, vol. 1, pp. 303–320.
11. Guo, Z.Y. and Li, Z.X., Size Effect on Single-Phase Channel Flow and Heat Transfer at Microscale, *Int. J. Heat Fluid Flow*, 2003, vol. 24, pp. 284–298.
12. Celata, G.P., Cummo, M., Marconi, V., Mcphail, S.J., and Zummo, G., Microtube Liquid Single-Phase Heat Transfer in Laminar Flow, *Int. J. Heat Mass Transfer*, 2006, vol. 49, pp. 3538–3546.
13. Peng, X.F., Peterson, G.P., and Wang, B.X., Frictional Flow Characteristics of Water Flowing through Rectangular Microchannels, *Exp. Heat Transfer*, 1994, vol. 7, pp. 249–264.
14. Peng, X.F., Peterson, G.P., and Wang, B.X., Heat Transfer Characteristics of Water Flowing through Microchannels, *Exp. Heat Transfer*, 1994, vol. 7, pp. 265–283.
15. Sobhan, C.B. and Garimella, S.V., A Comparative Analysis of Studies on Heat Transfer and Fluid Flow in Microchannels, *Microscale Therm. Eng.*, 2001, vol. 5, no. 4, pp. 293–311.
16. Steinke, M.E. and Kandlikar, S.G., Single-Phase Liquid Friction Factors in Microchannels, *Int. J. Therm. Sci.*, 2006, vol. 45, pp. 1073–1083.
17. Pfahler, J., Harley, J., Bau, H., and Zemel, J., Liquid Transport in Micron and Submicron Channels, *Sensors Actuators*, 1990, vol. 22, pp. 431–434.
18. Yu, D., Warrington, R., Barron, R., and Ameel, T., An Experimental and Theoretical Investigation of Fluid Flow and Heat Transfer in Microtubes, *ASME/JSME Therm. Eng. Conf.*, 1995, vol. 1, no. 52, pp. 523–530.
19. Adams, T.M., Abdel-Khalik, S.I., Jeter, S.M., and Qureshi, Z.H., An Experimental Investigation of Single-Phase Forced Convection in Microchannels, *Int. J. Heat Mass Transfer*, 1998, vol. 41, no. 6, pp. 851–857.
20. Mala, G.M. and Li, D.Q., Flow Characteristics in Microtubes, *Int. J. Heat Fluid Flow*, 1999, vol. 20, no. 2, pp. 142–148.
21. Lelea, D., Nishio, S., and Yakano, K., The Experimental Research on Microtube Heat Transfer and Fluid Flow of Distilled Water, *Int. J. Heat Mass Transfer*, 2004, vol. 47, no. 12, pp. 2817–2830.
22. Yang, C.Y., Chen, C.W., Lin, T.Y., and Kandlikar, S.G., Heat Transfer and Friction Characteristics of Air Flow in Microtubes, *Exp. Therm. Fluid Sci.*, 2012, vol. 37, pp. 12–18.
23. Harms, T.M., Kazmierczak, M.J., and Gerner, F.M., Developing Convective Heat Transfer in Deep Rectangular Microchannels, *Int. J. Heat Fluid Flow*, 1999, vol. 20, no. 2, pp. 149–157.
24. Liu, J.T., Peng, X.F., and Wang, B.X., Variable-Property Effect on Liquid Flow and Heat Transfer in Microchannels, *J. Chem. Eng.*, 2008, vol. 141, no. 1, pp. 346–353.
25. Liu, J.T., Peng, X.F., and Yan, W.M., Numerical Study of Fluid Flow and Heat Transfer in Microchannel Cooling Passages, *Int. J. Heat Mass Transfer*, 2007, vol. 50, no. 9, pp. 1855–1864.
26. Mahulikar, S.P. and Herwig, H., Physical Effects in Laminar Microconvection due to Variations in Incompressible Fluid Properties, *Phys. Fluids*, 2006, vol. 18, no. 7, pp. 1–12.
27. Herwig, H. and Mahulikar, S.P., Variable Property Effects in Single-Phase Incompressible Flows through Microchannels, *Int. J. Therm. Sci.*, 2006, vol. 45, no. 10, pp. 977–981.
28. Mahulikar, S.P., Herwig, H., Hausner, O., and Kock, F., Laminar Gas Microflow Convection Characteristics due to Steep Density Gradients, *Europhys. Lett.*, 2004, vol. 68, no. 6, pp. 811–817.
29. Mahulikar, S.P. and Herwig, H., Physical Effects in Pure Continuum-Based Laminar Microconvection due to Variations of Gas Properties, *J. Phys. D: Appl. Phys.*, 2006, vol. 39, no. 18, pp. 4116–4123.
30. Gulhane, N.P. and Mahulikar, S.P., Variations in Gas Properties in Laminar Microconvection with Entrance Effect, *Int. J. Heat Mass Transfer*, 2009, vol. 52, no. 7, pp. 1980–1990.

31. Gulhane, N.P. and Mahulikar, S.P., Numerical Investigation on Laminar Microconvective Liquid Flow with Entrance Effect and Graetz Problem due to Variations in Thermal Properties, *Heat Transfer Eng.*, 2012, vol. 33, no. 8, pp. 748–761.
32. Mahulikar, S.P. and Herwig, H., Fluid Friction in Incompressible Laminar Convection: Reynolds' Analogy Revisited for Variable Fluid Properties, *Eur. Phys. J. B: Condensed Matter Complex Syst.*, 2008, vol. 62, no. 1, pp. 77–86.
33. Gulhane, N.P. and Mahulikar, S.P., Numerical Study of Compressible Convective Heat Transfer with Variations in All Fluid Properties, *Int. J. Therm. Sci.*, 2010, vol. 49, no. 5, pp. 786–796.
34. Gulhane, N.P. and Mahulikar, S.P., Numerical Study of Microconvective Water-Flow Characteristics with Variations in Properties, *Nanoscale Microscale Therm. Eng.*, 2011, vol. 15, no. 1, pp. 28–47.
35. Nonino, C., Giudice, S. Del, and Savino, S., Temperature-Dependent Viscosity Effects on Laminar Forced Convection in the Entrance Region of Straight Ducts, *Int. J. Heat Mass Transfer*, 2006, vol. 49, no. 23, pp. 4469–4481.
36. Nonino, C., Giudice, S. Del, and Savino, S., Temperature-Dependent Viscosity and Viscous Dissipation Effects in Microchannel Flows with Uniform Wall Heat Flux, *Heat Transfer Eng.*, 2010, vol. 31, no. 8, pp. 682–691.
37. Giudice, S. Del, Nonino, C., and Savino, S., Effects of Viscous Dissipation and Temperature-Dependent Viscosity in Thermally and Simultaneously Developing Laminar Flows in Microchannels, *Int. J. Heat Fluid Flow*, 2007, vol. 28, no. 1, pp. 15–27.
38. Giudice, S. Del, Savino, S., and Nonino, C., Temperature-Dependent Viscosity and Thermal Conductivity Effects on the Laminar Forced Convection in Straight Microchannels, *J. Heat Transfer*, 2013, vol. 135, no. 10, pp. 1–8.
39. Giudice, S. Del, Savino, S., and Nonino, C., Entrance and Temperature-Dependent Property Effects in the Laminar Forced Convection in Straight Ducts with Uniform Wall Temperature, *J. Phys.: Conf. Ser.*, 2014, vol. 501, pp. 1–9.
40. Kumar, R. and Mahulikar, S.P., Effect of Temperature-Dependent Viscosity Variation on Fully Developed Laminar Microconvective Flow, *Int. J. Therm. Sci.*, 2015, vol. 98, pp. 179–191.
41. Kumar, R. and Mahulikar, S.P., Frictional Flow Characteristics of Microconvective Flow for Variable Fluid Properties, *Fluid Dyn. Res.*, 2015, vol. 47, pp. 1–21.
42. Holman, J.P., *Heat Transfer*, New York: McGraw-Hill, 1990.
43. Sherman, F.S., *Viscous Flow*, New York: McGraw-Hill, 1990.